Internal Waves, Bottom Slopes and Boundary Mixing

G.N. Ivey, P. De Silva and J. Imberger

Department of Environmental Engineering, Centre for Water Research, University of Western Australia, Nedlands, Western Australia, 6009.

Abstract: Laboratory experiments in continuously stratified fluids with internal waves breaking on planar bottom slopes indicate that while mixing is most intense near the local critical frequency ω_c, contributions to mixing are observed over the frequency range where $0.5 < \omega/\omega_c < 2.5$. For the critical case when the turbulence is most energetic, the turbulent benthic layer is not well mixed. The benthic layer varies in thickness over a wave cycle and the laboratory data indicate the mean thickness h is 15% of the wavelength of the incident wave, measured perpendicular to the slope. A simple model relates the mean rate of dissipation of turbulent kinetic energy $\bar{\varepsilon}$ and the diffusivity K within the benthic layer to the properties of the incident wave field, and yields a simple criterion for a buoyancy flux to occur within the benthic layer. Even though this criterion appears to be readily satisfied in the field, available observations do not yield clear evidence of a buoyancy flux. The turbulent activity in the benthic layers on the sloping bottoms therefore must be significant for the chemical and biological productivity, but the consequences for basin scale mixing in either lakes or the oceans are as yet undetermined.

Introduction

The dynamics of the turbulent benthic boundary layers and their role in mixing and transport processes on the basin scale have long been an area of great interest, particularly since Munk (1966) suggested that mixing at the boundaries could be responsible for the basin scale vertical mixing. Much attention has since been focussed on mixing at the boundaries, e.g., in recent review articles by Garrett, MacCready and Rhines (1993) and by Imberger (1994), with application to oceanography and limnology, respectively.

Models of the near boundary flows resulting from turbulence near a sloping bottom have been proposed (e.g., Phillips *et al.* 1986, Garrett 1990, Salmun *et al.* 1991) based on assumptions about the distribution of turbulent diffusivity with height above the bottom. Imberger and Ivey (1993) showed that a number of flow regimes were in fact possible, depending on the relative magnitudes of two ordering parameters: the Grashof number $Gr = (g\Delta\rho h^3/\rho_0 K^2)\cos\beta$ and the aspect ratio $A = h/L << 1$. In their formulation the benthic layer was assumed well-mixed over a depth h, $\Delta\rho$ was the density anomaly between the well-mixed boundary layer and the interior, L the along-slope scale characterising the background density gradient variability, β the bottom slope, and K the eddy diffusivity within the benthic layer, assumed the same for momentum and species. Using a perturbation solution in the small parameter A, they argued that in the flow regime likely to be relevant to lakes when $Gr = O(A^{-3/2})$, the interior vertical eddy diffusivity K_I at the depth of the density gradient extremum was given by

$$K_1 = \left(8\times10^{-6}\right)\frac{N^4 h^9 \sin^3\beta\cos^2\beta}{K^3 L_B} \qquad (1)$$

where L_B is the horizontal basin dimension and N is the maximum value of the buoyancy frequency in the thermocline.

In order to utilise such models, one therefore needs a knowledge of both the readily determinable geometrical properties of a basin, such as the bottom slope and basin size, but also two properties of the flow field: the benthic layer thickness h and the turbulent diffusivity K. As eq. (1) illustrates, the interior diffusivity K_I is particularly sensitive to the choice of either parameter, a conclusion which holds no matter what flow regime governs the dynamics of the benthic layer on the slope. The specification of the these two flow parameters is the issue we wish to address in the present work, and our focus here is on the mechanisms driving mixing at the boundary and how they influence h and K.

While the near boundary mixing can be driven by a mean flow over the hydraulically rough boundary, the more likely mechanism for driving boundary mixing is due to the interaction of the internal wave field with the sloping bottom - an observation which has motivated a number of laboratory studies (e.g., Ivey and Nokes 1989, Taylor 1993, De Silva *et al.* 1995) and field studies (e.g., Eriksen 1985, Eriksen 1995, Thorpe *et al.* 1990, Van Haren *et al.* 1994).

Laboratory Experiments

There have been three laboratory studies which have investigated breaking internal waves on slopes with a monochromatic incident internal wave: an initial study by Ivey and Nokes (1989,1990) conducted on a 30° bottom slope and over a range of incident frequencies around the critical frequency ω_c (group velocity vector of the reflected wave parallel to the bottom slope); a study by Taylor (1993) on a 20° bottom slope and confined to the critical frequency; and a study by De Silva *et al.*

(1995) on a 20° bottom slope using a very different configuration for generating internal waves and focusing on the frequency range above the critical frequency.

Ivey and Nokes (1989) showed that at the critical frequency a turbulent benthic boundary layer formed along the bottom. The thickness of the benthic layer h varied over the wave cycle, with maximum thickness during the upslope phase of the motion. The turbulence intensity in the layer also appeared to vary, although no direct measurements were made of turbulence properties. Sustained forcing over many wave cycles led to a change in potential energy P of the fluid in the laboratory tank. The average mixing efficiency in the benthic region over a wave cycle defined as $R_f = P/W$, where W was the net energy input into the benthic region, was dependent on wave amplitude but had a maximum value of $R_f = 0.2$, indicating the process can be quite efficient compared to other mixing mechanisms (e.g. Ivey and Imberger 1991). As seen in Figure 1, the mixing efficiency also varies with frequency ω with the maximum near the critical frequency ω_c but still a significant contribution coming from a bandwidth in the range $0.7 < (\omega/\omega_c) < 1.8$. For a typical internal wave spectrum in the ocean or lake, the implication is that even though the mixing efficiency is lower away from the local critical frequency, there can still be a significant contribution to mixing, particularly for the sub-critical frequencies with higher energy levels.

Taylor (1993) extended these experiments to a lower bottom slope of 20° and, by examining the microstructure signals in the boundary layer, confirmed that the turbulence intensity varied in intensity over a wave cycle. The most intense mixing occurred on the upslope phase of the wave cycle - as also observed in the field observations reported by White (1994) and Van Haren *et al.* (1994), for example. Mixing efficiencies were slightly smaller but comparable to those reported by Ivey and Nokes (1989). The direct numerical simulations reported by Slinn and Riley (1994) were the first to examine the case of critical waves on very low slopes down to 3.4°. Their results suggested that for steep slopes (defined to be greater than 20°) the mixing appeared nearly continuous over the wave cycle, while for shallow slopes (defined to be less than 10°) the mixing was more intermittent in nature over a wave cycle. Mixing efficiencies were reported as high as 0.39, but as there are differences in the definition between the numerical calculation and the laboratory experiments, it is difficult to draw definitive conclusions. From measurements of the velocity field, Taylor (1993) observed a strong interaction between the upslope and downslope flow and concluded that the mechanism generating the turbulence was not simply described by either a simple shear flow or a convective type instability, but had elements of both depending on the phase of the wave cycle and position relative to the bottom.

These early experiments had used a flap wavemaker at one end of a long channel which produced a wave with wavelength comparable to the slope length. The flow field was more in the nature of flow in a horizontal duct rather than a discrete wave ray impinging on an infinite planar slope. Recently, De Silva *et al.* (1995) have used a rather different means of generating the internal wave as shown schematically in Figure 2. The configuration has the advantage of producing an internal wave ray with wavelength small compared to the length scale of the slope and minimises the potential geometrical dependence introduced by the presence of the wedge shaped region at the top of the slope, of particular importance to the study of supercritical wave reflection.

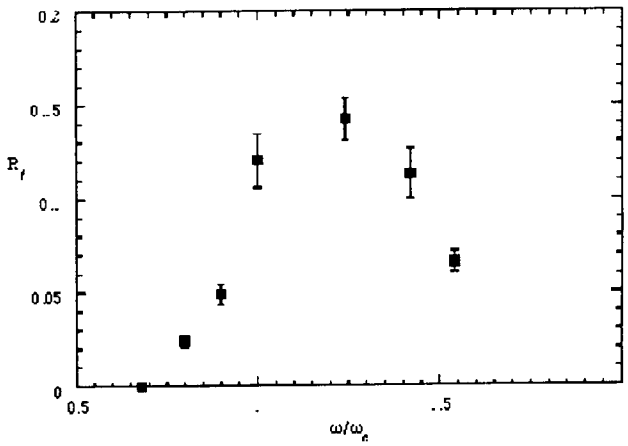

Figure 1. Cycle averaged mixing efficiencies as a function of forcing frequency where the incident wave amplitude is fixed in all cases. Paddle amplitude A = 2.2 cm and β = 30.

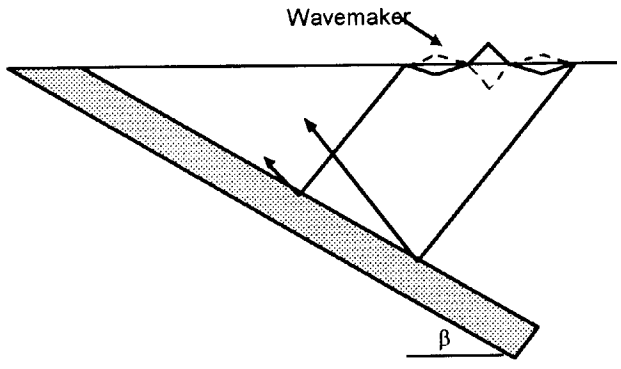

Figure 2. Schematic of horizontal articulated internal wave maker as employed by Teoh *et al.* (1995) and De Silva *et al.* (1995). Wavemaker is arranged so there is zero net displacement at the surface and a confined wave ray, of horizontal scale 1.5 wavelengths, is directed down onto the sloping bottom.

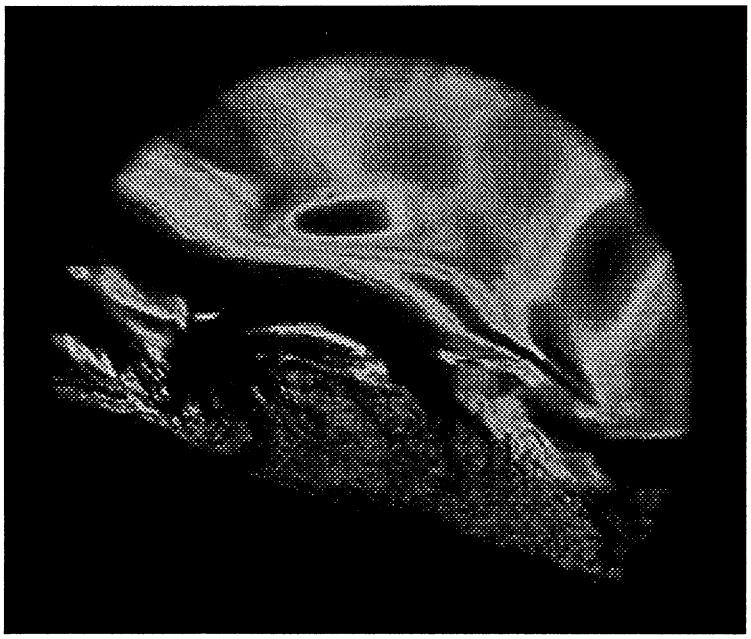

(a)

(b)

Figure 3. Rainbow schlieren images of breaking internal waves taken just after mixing has initiated. In Figure 3a, $\omega/\omega_c = 2.07$ and in Figure 3b $\omega/\omega_c = 2.43$. In both cases the incident wave amplitude is 2 cm.

In Figure 3 we show two rainbow schlieren images of the waves breaking on the slope. The schlieren technique used is described in some detail by Ivey and Nokes (1989), and the optical arrangement used here is identical. In Figure 3a we show the case where ω/ω_c = 2.07 with the incident ray coming in from the top right and reflecting forward toward shallow water on the left, and the image is taken a few cycles after the initiation of paddle motion. Even at this relatively high forcing frequency compared to the critical frequency, a mixing region is observed which has developed at the slope itself and extends along the slope a distance of the width of the incoming ray. Conversely at the higher forcing frequency in Figure 3b where ω/ω_c = 2.43, the mixing region has been established off the slope and there is a laminar region immediately adjacent to the slope. With continual wave forcing, the mixing region grows and extends down to the bottom. Thorpe (1987) has shown that non-linear second and third order resonances can occur between incident and reflected waves, which lead to regions of static instability off the slope, reminiscent of what is shown in Figure 3b. However, the theory predicts this should only occur for bottom slopes $\beta < 10^0$, considerably less than the 20° in figure 3, so the explanation of this observation is not yet clear. Note also that mixing is occurring at a range beyond that shown in Figure 1, implying that if there is enough energy available in the incident wave field at a given frequency, mixing can occur over a surprisingly broad bandwidth.

In Figure 4 we show some typical results of microstructure profiles over the depth. Note that the resolution of measurements made with the conductivity and temperature probes is comparable with that of the schlieren system which is able to resolve spatial scales down to about 0.7 mm (Taylor 1993). From the density profiles which extend to within 5 mm of the bottom, while there is variability during the wave cycle there is no evidence of any persistent well mixed regions close to the bottom. If we take the turbulent benthic region as the height at which overturning scales shown in the second panel disappear, the benthic layer is about 10 cm thick - consistent with the visual observations in Figure 3. Note also that the turbulence intensity does vary over the cycle where even the largest displacement scales are, at most, about 20% of the total thickness of the benthic region.

Mixing in the benthic region

These observations suggest the following simple mixing model. Consider the configuration shown in Figure 2. For an internal wave train in two dimensions, linear theory (e.g. Phillips 1977) indicates the velocity and density perturbations are described by

$$w = \alpha \cos\theta \cos(kx + nz - \omega t)$$

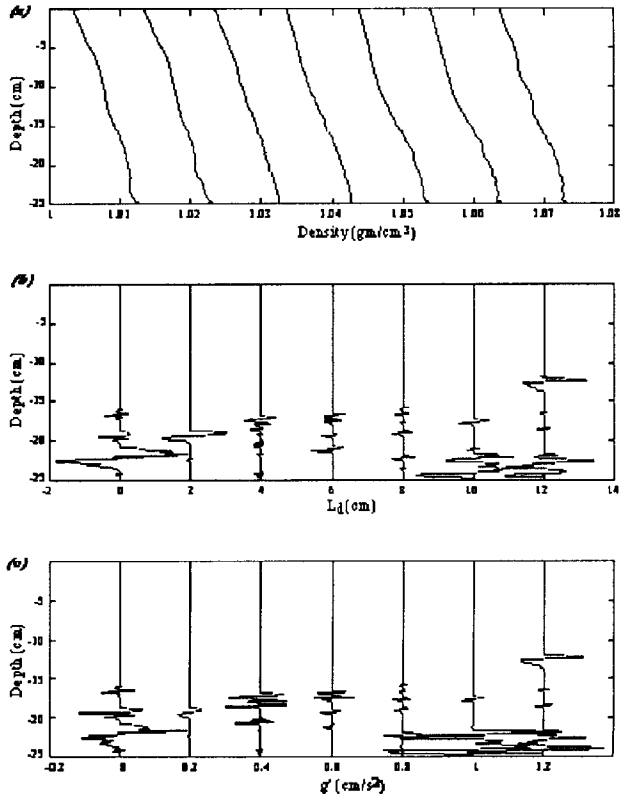

Figure 4. Microstructure profiles through a typical wave cycle once mixing has been initiated. Parameters are N = 0.64 rs^{-1}, ω = 0.45 rs^{-1}, wave amplitude 2.9 cm. Profiles are at intervals of 0.14 ($2\pi/\omega$). In the first panel, all profiles are displaced by 0.01 gm/cm^3 from the first profile. The second panel shows sample displacement scales and the third panel the corresponding buoyancy anomaly g'.

$$u = -\alpha \sin\theta \cos(kx + nz - \omega t) \qquad \text{(2a.b.c)}$$

$$\rho = -\frac{\alpha}{g\omega}\rho_0 N^2 \cos\theta \sin(kx + nz - \omega t)$$

where u and w are the horizontal and vertical velocities (x and z direction, respectively), k and n are the horizontal and vertical wavenumbers, ρ is the density perturbation, α is the maximum particle speed and θ the angle of the group velocity vector to the horizontal. The average over one wave period of the vertical energy flux passing though a horizontal surface with dimensions of one wavelength in the x direction and unit width in the y direction is

$$\dot{E}_i = \frac{\pi}{k}\rho_0 \alpha^2 C \sin\theta \qquad (3)$$

where C is the phase speed.

When the waves are incident on a bottom of slope β, the reflected energy is in general given by $\dot{E}_r = (1-r)\dot{E}_i$, (where the reflection coefficient $r = 0$ for perfect reflection). On the basis of the laboratory observations of Ivey and Nokes (1989), Taylor (1993) and De Silva *et al.* (1995), it seems reasonable to assume that for the case of critical wave reflection, once a turbulent mixing layer is established along the bottom, no energy is reflected at the incident or at any other frequency - due to dispersion in the frequency content resulting from mixing in the turbulent region, for example.

Then for the critical case, the average dissipation over one wave cycle is

$$\bar{\varepsilon} = \frac{\dot{E}_i}{M} = \frac{\dot{E}_i}{\rho_0 h l} \tag{4}$$

where M is the mass of fluid (per unit width) in which the incident wave energy is dissipated, h is the average thickness of the benthic layer and l is the along-slope length over which mixing is occurring.

In Figure 5a we plot the observed values of boundary layer thickness h obtained by Ivey and Nokes (1989) against the Reynolds number based on incident wave properties. It is apparent that above a minimum Reynolds number of about 50, the observed value of boundary thickness h is remarkably constant in the range of (0.10 - 0.15)λ_v, where λ_v is the wavelength of the incident wave measured perpendicular to the slope. In Figure 5b, we plot similar observations from De Silva *et al.* (1995), and while the data set is small it appears $h \approx 0.15\lambda_v$ for supercritical waves as well although there may also be some dependence on wave amplitude. These results are also consistent with the experiments of Taylor (1993) (see his Figure 3, for example), and the field data of Van Haren *et al.* (1994) and White (1994), although smaller than the values found by Slinn and Riley (1994).

If we take the benthic layer thickness as $h = 0.15\lambda_v$ then this can be written as

$$h = 0.15\left(\frac{2\pi}{\sqrt{k^2+n^2}\cos 2\beta}\right) \tag{5}$$

Substituting (5) into (4) and noting from the geometry that $l = \pi / (k \cos \beta)$, we obtain

$$\bar{\varepsilon} = \left(\frac{3\alpha^2 N}{4\pi}\right)\sin 4\beta\cos\beta \tag{6}$$

Using the result from Osborn (1980), the eddy diffusivity for the stratifying species in the benthic boundary layer can thus be written as

$$K = \left(\frac{R_f}{1-R_f}\right)\left(\frac{3\alpha^2}{4\pi N}\right)\sin 4\beta\cos\beta \tag{7}$$

A necessary condition for the turbulence to be sufficiently energetic to sustain a buoyancy flux is $\bar{\varepsilon}/\nu N^2 > 15$(e.g. Ivey and Imberger 1991), where ε is the instantaneous dissipation rate. Cycle averaged values (e.g. Ivey and Nokes 1989, Taylor 1993) are about a factor of two lower than this, so a conservative estimate would say $\bar{\varepsilon}/\nu N^2 > 15$ is a necessary condition for a buoyancy flux.

Ivey and Imberger (1991) also demonstrated that the value of the mixing efficiency R_f depends strongly on the turbulent Froude Number defined as $Fr_T = (L_o/L_c)^{2/3}$, where the Ozmidov scale $L_o = (\varepsilon/N^3)^{1/2}$ and the displacement scale is L_c. If $Fr_T = 1$, then the mixing is highly efficient with $R_f = 0.2$, but for values of Fr_T either above or below $Fr_T = 1$, the value of R_f decreases rapidly. Laboratory observations (De Silva *et al.* 1995) and field observations (see below) indicate that $Fr_T = 1$ only occasionally and it appears to vary greatly from profile to profile.

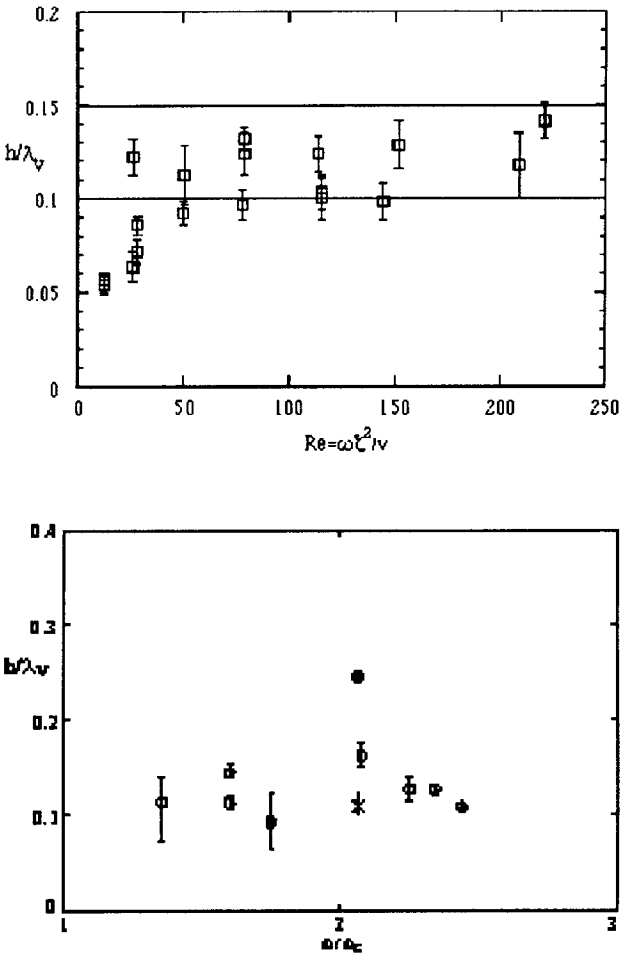

Figure 5. Measurements of boundary layer thickness obtained from schlieren images. (top) panel shows data from Ivey and Nokes (1989) where ζ is wave amplitude. (bottom) panel shows data from experiments by De Silva et al. (1995) in the configuration shown in Figure 2.

It is tempting to generalise the arguments above to the case of non-critical reflection where $0<r<1$, hence (6) becomes

$$\bar{\varepsilon} = r\left(\frac{3\alpha^2 N}{4\pi}\right)\sin 4\beta\cos\beta \qquad (8)$$

Javam *et al.* (1995), for example, have examined the reflection of an internal wave at a critical level, and find the reflection coefficient varies between 0.2 to 1.0, depending on the Reynolds number. Comparable calculations thus need to be made for waves reflecting off the bottom when a turbulent mixing region is present in order to utilize (8).

Field observations

Using data from Lake Biwa, Japan, Imberger (1994) demonstrated that in order to explain the typical internal wave spectral levels and relatively rapid decay of large scale internal waves, generated by aperiodic wind events for example, the benthic boundary regions must be regions of very high dissipation compared to the interior - at least two orders of magnitude larger than typical interior levels of dissipation of order 10^{-9} m^2 s^{-3}. In the ocean, Eriksen (1985) estimated that 8% of the Garrett Munk internal wave energy flux had to be converted to potential energy to yield Munk's (1966) canonical interior vertical diffusivity of 10^{-4} m^2 s^{-1}. More recent calculations (e.g. Gilbert and Garret 1989) and measurements (e.g. Eriksen 1995) imply values an order of magnitude less than this seem more likely. Only recently have observations been made which have attempted to link the internal wave field, near boundary turbulence and the resulting buoyancy flux.

Thorpe *et al.* (1990) and White (1994) describe results from the Hebrides Slope, where the M_2 internal tide is locally critical to the bottom slope, which show clear evidence of enhanced mixing on the upslope phase of motion, and much weaker mixing in the downslope phase, as seen in the laboratory experiments. With a local vertical wavelength of about 1 km, White (1994) shows evidence of mixing up to and including their last instrument at 110 m off the slope - consistent with the laboratory prediction of benthic layer thickness in Figure 5a. Van Haren *et al.* (1994) find benthic layers of height of thickness 10 m when the local vertical wavelength was 120 m. Intriguingly, while their dissipation estimates indicate that $\bar{\varepsilon}/\nu N^2 \approx 400$, they were unable to find any evidence for significant buoyancy fluxes.

Eriksen's (1995) observations from Fieberling Guyot seamount in the North Pacific clearly show significant levels of enhanced activity near the local critical frequency of 0.42 cph where N = 1.02 cph (i.e. $\beta = 24°$). With a vertical wavelength of 3 km, equation (5) predicts turbulent activity up to a level of some 450 m off the bottom, although this is clearly an oversimplification of the issue for such large vertical wavelengths. Such a steep bottom slope would suggest relatively continuous mixing over a wave cycle. Taking $\beta = 24°$, N = 1.02 cph and taking as the incident wave field the background GM spectrum close to the bottom, we obtain (e.g. Eriksen 1995 figure 3a) $\alpha \approx 0.5$ cm s^{-1}, and hence from (6) $\bar{\varepsilon} = 1\times10^{-8}$ m^2 s^{-3}. Toole *et al.* (1994) report direct microstructure measurements near the base of Fieberling Guyot. Their results clearly show an increase in dissipation as the bottom is approached with the deepest estimate, still some 500 m off the bottom, having a value of $\varepsilon = 10^{-9}$ m^2 s^{-3}.

Microstructure measurements in the benthic boundary layer in Lake Kinneret, Israel have been reported by Imberger *et al.* (1995). One of the most striking features of their results shown in Figure 6 is the considerable variation in the turbulent Froude number Fr_T. Many events occur which have Froude numbers very different than one, implying the mixing efficiency R_f is very small and the events have little or no buoyancy flux associated with them. The implication is that even if the dissipation is significant compared to background levels, the buoyancy flux or species diffusivity K, may be negligibly small.

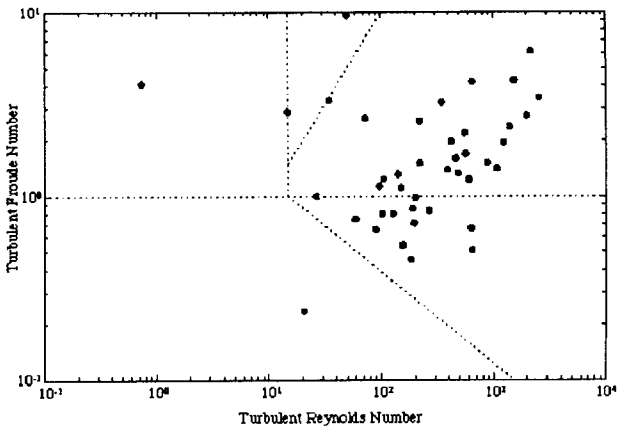

Figure 6. Microstructure measurements in the benthic boundary layer in Lake Kinneret, Israel from Imberger *et al.* (1995). Data plotted on an activity diagram where the Turbulent Froude number $Fr_T = (L_o/L_c)^{2/3}$ and the Turbulent Reynolds number $Re_T = (L_c/L_k)^{4/3}$. The Ozmidov scale $L_o = (\varepsilon/N^3)^{1/2}$ is based on the re-sorted density profile, L_k is the Kolmogorov scale and L_c is the displacement scale.

Conclusions

Recent laboratory experiments give some insight into the dynamics of the turbulent mixing region that can form along a sloping bottom boundary in a continuously stratified fluid where mixing is driven by breaking

internal waves. Using a simple model, it is possible to obtain expresions for the benthic layer thickness h and the turbulent diffusivity K within this benthic region in terms of the properties of the incident wave field. Further laboratory and numerical experiments need to be conducted, particularly for non-critical waves, to test the validity of these expressions. Both in the laboratory and the field, care is needed in distinguishing between the measurements made from instantaneous measurements and values valid over one wave cycle and longer.

While the evidence so far is hardly conclusive, it may transpire that the benthic layer on the sloping bottom is one of enhanced turbulent dissipation but with a negligible turbulent buoyancy flux. This has significant implications for circulation modelling and for the chemistry and biological processes near the boundary in lakes and the ocean (cf. Imberger 1994). Such a scenario does explain one obvious feature of lakes: they stay stratified unless seasonal cooling occurs. Only careful experiments in the future will enable these questions to be answered.

This work is supported by the Australian Research Council. Environmental Dynamics Report ED 807 GI.

References

De Silva, P., G.N. Ivey, and J. Imberger, 1995: Turbulence and mixing due to breaking internal waves on sloping boundaries. in preparation.

Ericksen, C.C., 1985: Implications of ocean bottom reflection for internal wave spectra and mixing. *J. Phys. Oceanogr.*, 15, 1145-1156.

Ericksen, C.C., 1995: Internal wave reflection and mixing at Fieberling Guyot, *J. Geophys. Res.*, submitted.

Garrett, C., 1990: The role of secondary circulation in boundary mixing. *J. Geophys. Res.*, 95, 3181-3188.

Garrett, C., O. Macready, and P. Rhines, 1993: Boundary mixing and arrested Ekman layers: rotating stratified flow near a sloping boundary. *Ann. Rev. Fuid Mech.*, 19, 1716-1729.

Gilbert, D. and C. Garrett, 1989: Implications for ocean mixing of internal wave scattering off irregular topography. *J. Phys. Oceanogr.*, 19, 1716-1729.

Imberger, J. and G.N. Ivey, 1993: Boundary mixing in stratified reservoirs. *J. Fluid Mech.*, 183, 25-44.

Imberger, J., 1994: Transport processes in lakes: a review. in *Limnology Now: a Paradigm of Planetary Problems*. R. Margalef (ed.), Elsevier, 99-193.

Imberger, J., T. Zohary, and C. Thomson, 1995: Boundary mixing in lakes. in preparation.

Ivey, G.N. and R.I. Nokes, 1989: Mixing driven by the breaking of internal waves against sloping boundaries. *J. Fluid Mech.*, 204, 479-500.

Ivey, G.N., and R.I. Nokes, 1990: Mixing driven by the breaking of internal waves against sloping boundaries. In *Proc. Intl. Conf. Physical Modelling of Transport and Dispersion*, M.I.T., Cambridge, Mass., 11A.3-11A.8

Ivey, G.N., and J. Imberger, 1991: On the nature of turbulence in a stratified fluid, Part 1: The efficiency of mixing. *J. Phys. Oceanogr.*, 21, 650-658.

Javam, A., S.W. Armfield, and J. Imberger, 1995: Numerical study of internal wave generation in a stratified fluid. *J. Fluid Mech.*, submitted.

Munk, W. H., 1966: Abyssal recipes. *Deep Sea Res.*, 13: 207-230.

Osborn, T.R., 1980: Estimates of the local rate of vertical diffusion from dissipation measurements. *J. Phys. Oceanogr.*, 10, 83-89.

Phillips, O.M., 1977: The dynamics of the upper ocean. Cambridge.

Phillips, O.M., J.-H. Shyu, and H. Salmun, 1986: An experiment on boundary mixing: mean circulation and transport rates. *J. Fluid Mech.*, 173, 473-499.

Salmun, H., P.D. Killworth, and J.R. Blundell, 1991: A two-dimensional model of boundary mixing. *J. Geophys. Res.*, 96, 18,447-18,474.

Slinn, D.N., and J.J. Riley, 1994: Turbulent mixing in the oceanic boundary layer due to internal wave reflection from sloping terrain. in *Proc. 4th International Symp. Stratified Flows*, Grenoble, France, to appear.

Taylor, J., 1993: Turbulence and mixing in the boundary layer generated by shoaling internal waves. *Dyn. Atmos. Oceans.*, 19, 233-258.

Thorpe, S.A., 1987: On the reflection of a train of finite-amplitude internal waves from a uniform slope. *J. Fluid Mech.*, 178, 279-302.

Thorpe, S.A., P. Hall, and M.White, 1990: The variability of mixing on a continental slope. *Proc. Roy. Soc.*, A439,115-130.

Teoh, S.G., G.N. Ivey, and J. Imberger, 1995: Observations of interactions between two internal wave rays. *J. Fluid Mech.* in preparation.

Toole, J.M., K.L. Polzin, and R.W. Schmitt, 1994: Estimates of diapycnal mixing in the ocean. *Science*, 264, 1120-1123.

Van Haren, H., N. Oakey, and C. Garrett , 1994: Measurements of internal wave band eddy fluxes above a sloping bottom. *J. Mar. Res.*, 52, 909-946.

White, M., 1994: Tidal and subtidal variability in the sloping benthic boundary layer. *J. Geophys. Res.*, 99, 7851-7864.